



Published in final edited form as:

Biomacromolecules. 2016 February 8; 17(2): 601–614. doi:10.1021/acs.biomac.5b01541.

Liposome-Cross-Linked Hybrid Hydrogels for Glutathione-Triggered Delivery of Multiple Cargo Molecules

Yingkai Liang[†] and Kristi L. Kiick^{†,‡,§,*}

[†]Department of Materials Science and Engineering, University of Delaware, Newark, Delaware 19716, United States

[‡]Department of Biomedical Engineering, University of Delaware, Newark, Delaware 19716, United States

[§]Delaware Biotechnology Institute, 15 Innovation Way, Newark, Delaware 19716, United States

Abstract

Novel, liposome-cross-linked hybrid hydrogels cross-linked by the Michael-type addition of thiols with maleimides were prepared via the use of maleimide-functionalized liposome cross-linkers and thiolated polyethylene glycol (PEG) polymers. Gelation of the materials was confirmed by oscillatory rheology experiments. These hybrid hydrogels are rendered degradable upon exposure to thiol-containing molecules such as glutathione (GSH), via the incorporation of selected thioether succinimide cross-links between the PEG polymers and liposome nanoparticles. Dynamic light scattering (DLS) characterization confirmed that intact liposomes were released upon network degradation. Owing to the hierarchical structure of the network, multiple cargo molecules relevant for chemotherapies, namely doxorubicin (DOX) and cytochrome c, were encapsulated and simultaneously released from the hybrid hydrogels, with differential release profiles that were driven by degradation-mediated release and Fickian diffusion, respectively. This work introduces a facile approach for the development of advanced, hybrid drug delivery vehicles that exhibit novel chemical degradation.

Graphical Abstract

*Corresponding Author. kiick@udel.edu; Tel.: +1 302 831 0201.

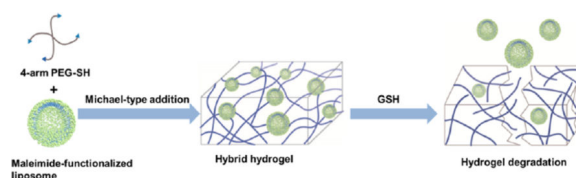
ASSOCIATED CONTENT

Supporting Information

The Supporting Information is available free of charge on the [ACS Publications website](https://pubs.acs.org) at DOI: 10.1021/acs.biomac.5b01541.

Dynamic rheology of the liposome-cross-linked hydrogels and PEG-SH polymer control, as well as non-maleimide liposome/polymer control, SEM image, DOX release profiles of PEG hydrogel control, data fitting of hydrogel degradation and DOX release profiles, Triton triggered release, and dialysis release of DOX from hybrid hydrogels, as well as equations and models for data fitting (PDF)

The authors declare no competing financial interest.



INTRODUCTION

Advances in nanotechnology have contributed significantly to the development of novel nanoscale carriers in the field of drug delivery.^{1–5} A wide variety of nanoparticles have been developed over the past few decades, including inorganic nanoparticles,^{6–8} liposomes,^{9–11} polymeric micelles,^{12–14} and nanogels.^{15–17} These nanoparticles are of appropriate size (10–150 nm) both to penetrate vessels and accumulate in specific tissues (e.g., tumors) and also for their surfaces to be functionalized with specific ligands for targeting effects, providing a promising platform for drug delivery with enhanced therapeutic efficacy.^{18–20} In particular, various liposomal formulations including both classical and stealth liposomes have been widely used in preclinical and clinical studies, with a number of drug-encapsulated liposomal products such as AmBisome and Doxil on the market and many more under clinical development.^{21,22} Parallel to the development of nanotechnology approaches in drug delivery, hydrogels have also been a focus of continued study as an important class of materials for the delivery of a variety of bioactive molecules including nutrients, drugs, and proteins.^{23–25} Composed of hydrophilic three-dimensional polymer networks, hydrogels have several advantageous properties including high water content, tunable viscoelasticity, and biocompatibility, which allow bioactive molecules to be protected against degradation and released from the hydrogel matrix in a controlled manner over an extended period of time.^{26,27} Among various kinds of polymeric hydrogels, hydrogels synthesized from polyethylene glycol (PEG), an FDA-approved polymer, have been extensively studied in the field of drug delivery and tissue engineering with encouraging preclinical and clinical results.^{26,28,29} Additionally, several PEG hydrogel-based medical devices composed of reactive PEG polymers including thiol-modified PEG and acrylate-modified PEG have received approval for use as sealants (CoSeal)³⁰ and wound healing matrices (Premvia).³¹

In recent years, there has been an increasing interest in the incorporation of nanoparticles into hydrogels for improved therapeutic efficacy.^{32–34} Such hybrid systems not only preserve the structural integrity and functionalities of the incorporated nanoparticles, but also combine the advantageous properties of two distinct drug delivery platforms, offering unique benefits such as improved tissue localization, minimized burst release, and controlled sequential delivery. A common approach for the preparation of these hybrid hydrogels is to trigger gelation of hydrogel-forming monomer solutions in nanoparticle suspensions. Varieties of nanoparticles including metallic nanoparticles,³⁵ carbon-based nanomaterials,³⁶ and polymeric nanoparticles³⁷ have been physically embedded within the hydrogel network to create reinforced polymeric hydrogels, developing nanocomposites with tailored physical properties and custom-made functionalities. Particularly, owing to their well-known advantages in drug delivery,³⁸ drug-loaded liposomes and modified liposome nanoparticles have been incorporated into a wide range of hydrogels based on synthetic polymers,^{39,40}

natural polymers,^{41,42} and peptides^{43,44} to provide prolonged release of the therapeutic molecules and significantly enhance therapeutic efficacy. Nevertheless, in these above cases, there is no specific interaction between the polymer matrix and the nanoparticle.

More recently, other strategies involving the use of nanoparticles as cross-linkers for hydrogel formation have been exploited,^{45–48} introducing additional engineering flexibility and structural diversity to these hybrid systems. For example, hydrophobic interactions between polymers and nanoparticles have been utilized to engineer self-assembled hydrogels with shear-thinning and self-healing properties. Raghavan and co-workers^{49–51} developed a series of injectable hybrid hydrogels based on the interactions between hydrophobically modified chitosan and various bilayer-structured building blocks (liposomes, vesicles, and cells). The hydrophobes from chitosan embedded in the hydrophobic interiors of the vesicle/cell bilayer membranes, forming hydrogels with shear-thinning behavior. Similarly, Langer and co-workers⁵² designed shear-thinning injectable hydrogels via the polymer–nanoparticle interactions between hydrophobically modified cellulose derivatives and hydrophobic nanoparticle surfaces. Additionally, polymer–nanoparticle hybrid hydrogels have also been fabricated via the covalent interactions between polymer chains and nanoparticle surfaces. Akiyoshi and co-workers^{53,54} reported biodegradable hybrid hydrogels based on the Michael-type addition between thiolated 4-arm polyethylene glycol (PEG) and acryloyl-modified pullulan nanogels. The PEG polymer chains covalently cross-linked the pullulan nanogels into a three-dimensional network, with the nanogels serving as structural components. These multicomponent hybrid hydrogels offer great opportunities for the sequential delivery of multiple drugs/growth factors, which improves therapeutic efficacy by synergistic effects that aid in overcoming drug resistance in cancer therapy^{11,55–58} and better mimic the temporal profile of the healing process during tissue regeneration.^{59,60} Despite the promise of these methods, nanoparticle-cross-linked hydrogels with chemo-responsiveness that is based on specific polymer–nanoparticle interactions have not been widely developed.^{48,61}

Inspired by these elegant approaches, we report an advanced, responsive drug delivery system that integrates liposome nanoparticles and PEG polymers into a unifying hydrogel construct for the controlled sequential delivery of multiple therapeutic molecules. Specifically, we have developed glutathione-sensitive, liposome-cross-linked hybrid hydrogels based on the reversible Michael-type addition between arylthiol-functionalized 4-arm PEG and maleimide-functionalized liposomes. The successful formation of the liposomes and liposome-cross-linked hydrogels was confirmed via dynamic light scattering (DLS) and oscillatory rheology. Mass loss and in vitro drug delivery experiments also confirmed that the selective capacity of certain thioether succinimides to undergo retro-Michael reaction and thiol exchange^{62–65} serves as the basis of cross-link scission between the PEG polymers and liposomes in thiol-containing microenvironments, resulting in matrix degradation and subsequent release of therapeutic molecules. The hierarchical structure of the gel enables dual encapsulation and differential release of multiple therapeutic cargos from one robust hybrid system with unique physical and chemical properties that are absent in the individual building blocks.

EXPERIMENTAL SECTION

Materials

4-Arm, alkylthiol-functionalized PEG (PEG-SH, M_n 20 000 g/mol) and 4-arm, hydroxyl-functionalized PEG (M_n 20 000 g/mol) were purchased from JenKem Technology USA, Inc. (Allen, TX, USA). All lipids were purchased from Avanti Polar Lipids (Alabaster, AL, USA), including: 1,2-dioleoyl-*sn*-glycero-3-phosphocholine (DOPC), anionic 1,2-dioleoyl-*sn*-glycero-3-phospho-(1'-rac-glycerol) (DOPG), and the anionic maleimide-functionalized lipid 1,2-dioleoyl-*sn*-glycero-3-phosphoethanolamine-N-[4-(*p*-maleimidophenyl)butyramide (MPB-PE). 4-Mercaptophenylpropionic acid (4-mercaptohydrocinnamic acid) was purchased from TCI America (Portland, OR, USA). Doxorubicin hydrochloride (DOX) was purchased from Alfa Aesar (Ward Hill, MA, USA). Glutathione (GSH) and cytochrome c from equine heart were purchased from Sigma-Aldrich (Saint Louis, MO, USA). All other reagents and materials were purchased from Fisher Scientific (Pittsburgh, PA, USA) unless otherwise noted. ^1H NMR spectra were acquired under standard quantitative conditions at ambient temperature on a Bruker AV400 NMR spectrometer (Billerica, MA, USA). All samples were dissolved in CDCl_3 (D, 99.8%) + 0.05% V/V TMS.

Synthesis of Arylthiol End-Functionalized 4-Arm PEG

The synthesis of arylthiolated 4-arm PEG was performed by modifying PEG with 4-mercaptohydrocinnamic acid based on a modified protocol from previous reports.⁶³ Briefly, 20K 4-arm PEG (2g, 0.4 mmol OH groups), 4-mercaptophenylpropionic acid (0.36g, 2 mmol), *p*-toluenesulfonic acid (*p*-TSA, 27.55 mg, 0.16 mmol), and dithiothreitol (DTT, 30.8 mg, 0.2 mmol) were dissolved in toluene (30 mL). The reaction mixture was refluxed at 155 °C with stirring for 48 h. Water was collected by using a Dean–Stark trap. The reaction mixture was precipitated in cold ether, and white polymer powder was collected after filtration. The polymer product was stored under N_2 at –20 °C for future use. ^1H NMR (400 MHz, CDCl_3): δ 7.22 (d, 2H), 7.10 (d, 2H), 4.27–4.21 (m, 2H), 3.67 (s, 449H), 2.92 (t, 2H), 2.65 (t, 2H).

Preparation of Maleimide-Functionalized Liposomes

The liposomes were prepared based on the conventional dehydration–rehydration method as previously reported.^{9–11} Ten micromoles of lipids in chloroform (a lipid composition of DOPC:DOPG:MPB = 4:1:5 molar ratio was typically used) were dispensed into small round-bottom flasks, and the organic solvents were evaporated under nitrogen overnight to prepare dried thin lipid films. The lipid films were rehydrated at room temperature in 1 mL 0.2 M bis-tris buffer at pH 7.0 for 1 h with rigorous vortexing for 30 s every 5 min, and then sonicated in alternating power cycles of 8% amplitude (~30W) in 30 s intervals for 5 min on ice. The resulting liposomes were extruded 21 times through a 0.2 μm polycarbonate membrane (Whatman, Piscataway, NJ, USA) using an Avanti Mini-Extruder (Avanti Polar Lipids Inc., Alabaster, AL, USA). The liposome solutions were freshly made and used shortly after preparation to avoid the ring-opening (hydrolysis) reactions of the maleimide moieties, which might prevent them from further reactions.⁶⁶ The average size of the monodisperse liposomes was analyzed via DLS at 25 °C on a Malvern Zetasizer Nano ZS

apparatus with Malvern Instruments DTS software (v.6.01) using the cumulants fit (Malvern Instruments, Malvern, Worcestershire, UK).

Preparation of Liposome-Cross-Linked Hybrid Hydrogels

The liposomal hybrid hydrogels were prepared by Michael-type addition between arylthiol end-functionalized 4-arm PEG and the maleimide-functionalized liposomes. Briefly, 20K 4-arm PEG arylthiol was dissolved directly in 10 mM liposome solutions (50 μ L, in 0.2 M bis-tris buffer at pH 7.0) at room temperature and the mixture was vortexed for approximately 30 s to completely dissolve the solid polymers. The mixture was then purged with nitrogen and incubated quiescently at 37 °C overnight to achieve complete cross-linking, although rheological experiments (below) confirm that gelation occurs within several minutes. The molar ratios of the maleimide groups from liposomes to the –SH groups from PEG were approximately 1:1, 1:2, and 1:4, which was altered by altering the amount of PEG-SH precursors added during preparation (3, 6, and 12 wt %, respectively). Thiol-insensitive hybrid hydrogels (control) were prepared by using 20K 4-arm, alkylthiol-functionalized PEG based on the same procedure. Detailed chemical structures of these thiolated PEG polymer precursors are included in Scheme 1. A PEG hydrogel-only control (without liposomes) was also prepared by dissolving 20K 4-arm PEG arylthiol and 10K 4-arm PEG maleimide in PBS separately and then mixing the two precursor solutions.

Rheological Studies

Oscillatory rheological characterization of the hybrid hydrogels was performed on a stress-controlled AR-G2 rheometer (TA Instruments, New Castle, DE, USA) equipped with a Peltier plate. In situ gelation experiments were conducted at 37 °C using a 20 mm-diameter, 1° cone and plate geometry with a 25 μ m gap distance, with oscillatory time, frequency, and strain sweeps performed. Strain sweeps were performed on samples from 0.1% to a maximum strain of 1000% to determine the limit of the linear viscoelastic region. Dynamic oscillatory time sweeps were performed to monitor the in situ gelation and mechanical properties of different hybrid hydrogel compositions at angular frequencies of 6 rad/s and 1% strain amplitude chosen from the linear viscoelastic region. Dynamic oscillatory frequency sweeps were conducted from 0.1 to 100 rad/s at 1% strain amplitude. Thiolated PEG polymer precursors were dissolved in the liposome suspension (~40 μ L). The mixture was then quickly vortexed and loaded onto the rheometer stage.

The results for PEG alkylthiol hydrogels instead of PEG arylthiol are shown for these in situ rheological experiments, as the arylthiol-based hydrogels showed frequency-responsive behaviors (likely resulting from the hydrophobic interaction between the aromatic moieties of PEG arylthiol and lipid bilayers) that complicated comparisons. For experiments to confirm the role of the liposomes in the mechanical integrity of the hydrogels, the hybrid hydrogels (~65 μ L) were formed in a 3 mL syringe prior to loading onto the rheometer stage, and then incubated in situ with 10% Triton X-100 in water at 37 °C. Dynamic oscillatory time sweeps were conducted at angular frequencies of 6 rad/s and 1% strain amplitude using an 8 mm-diameter, parallel plate geometry with a 200 μ m gap distance to monitor the changes in storage modulus when the hydrogels were immersed in 10% Triton X-100.

Scanning Electron Microscopy

The liposome-cross-linked hybrid hydrogels (~25 μL) were dehydrated in a series of ethanol/water solutions (1 mL) progressing from 30% ethanol to 50%, and 70% for 4 h respectively, and eventually to 100% ethanol for 12 h at room temperature. The dehydrated gels were dried at the critical point of CO_2 for 1 h using an Autosamdri-815B critical point dryer (Tousimis, Rockville, MD, USA). Samples were sputter coated with a thin layer of gold-palladium to provide a more conductive surface and imaged using scanning electron microscopy (SEM) at an accelerating voltage of 3.0 kV (Zeiss Auriga 60, Oberkochen, Germany).

Mass Loss Studies

Hydrogel samples were formed as described above by directly dissolving PEG-SH polymers (~3 mg) in liposome suspensions (~50 μL , in 0.2 M bis-tris buffer at pH 7.0) in 1.5 mL Eppendorf tubes and then incubating the mixture at 37 $^\circ\text{C}$ overnight. After being placed in phosphate buffered saline (PBS) for 24 h to achieve equilibrium swelling, the hydrogel samples were immersed in 1 mL 10 μM or 10 mM GSH solutions in PBS, or PBS alone at 37 $^\circ\text{C}$. At predetermined time points (every 48 h for the first 4 days and every 24 h after that until day 7), the mass of hydrogels after incubation was measured after blotting off excess water. The percentage of mass remaining from a hydrogel sample was calculated as [(mass after incubation)/(swollen mass)] \times 100%.

In Vitro DOX Encapsulation and Release

To prepare DOX-loaded liposomes, DOX was dissolved in a minimum amount of DMSO (ca. 10% of the total volume of liposome solutions, which were approximately 1 mL in volume) and added dropwise to the liposome suspensions (in 0.2 M bis-tris buffer at pH 7.0) while stirring, at a drug-to-lipid ratio of approximately 1:3. The mixture was stirred overnight at room temperature. The resulting DOX-loaded liposomes (usually in ~150 μL aliquots for each experiment), were used without further purification due to the small volume of the samples and the limited amount of unencapsulated DOX present (which was confirmed in DOX release experiments, see below). The encapsulation efficiency of DOX was indicated to be approximately 92%, and was determined by washing the DOX-loaded liposomes three times with PBS and then extracting the encapsulated DOX by treatment with 10% Triton X-100. A calibration curve for DOX was developed by measuring the fluorescence intensity of DOX solutions at a concentration range of 0.25–10 $\mu\text{g}/\text{mL}$ (excitation 485 nm, emission 590 nm) using a PerkinElmer Fusion microplate reader (Waltham, MA, USA).

DOX-loaded liposome-cross-linked hydrogels were prepared by dissolving either the aryl or alkylthiolated PEG polymers in DOX-loaded liposome suspensions. The resulting hydrogels (~50 μL) were then directly immersed in 1 mL 10 mM GSH in PBS solutions or PBS alone at 37 $^\circ\text{C}$. A volume of 0.5 mL of the supernatant was removed and replenished every day, and the release of DOX was monitored by measuring the fluorescence intensity (excitation 485 nm, emission 590 nm) of the removed buffer as described above.

Co-delivery of DOX and Cytochrome c in Vitro

DOX-loaded liposomes were prepared as described above, and the liposome suspensions (in 0.2 M bis-tris buffer at pH 7.0) were used to prepare hybrid hydrogels at 37 °C as above except with cytochrome c dissolved along with the arylthiol PEG polymers (potential side reactions including disulfide exchange between the protein and polymers are slow and thus expected to be insignificant within the time scale of the rapid cross-linking reaction),⁶⁷ with a total of 1 mg cytochrome c in 50 μ L of hydrogel to ensure detection upon release and to measure release at a high concentration gradient. The hydrogels were placed in 1.5 mL Eppendorf tubes, and 10 mM GSH in PBS (1 mL) was added to immerse the hydrogels. The hydrogels were incubated at 37 °C, and 0.5 mL of the supernatant was removed and replaced with fresh buffer every 24 h. The amount of cytochrome c was determined using a Pierce Microplate BCA Protein Assay Kit - Reducing Agent Compatible (Thermo Scientific, Rockford, IL, USA). The amount of DOX released was measured by fluorescence intensity using a microplate reader.

Data Analysis

Statistical analysis was performed using a two-tailed Student's *t* test. A *p* value of <0.05 was considered to be statistically different.

RESULTS AND DISCUSSION

Hydrogel Design

Maleimide-functionalized liposomes (10 mM, $D_H \sim 100$ nm according to DLS measurements) were prepared by the conventional hydration of dried lipid thin films (the total lipids comprised 50% by mole of a maleimide-functionalized lipid, MPB-PE, as well as 40% DOPC and 10% DOPG, Scheme 1A). Previous work reported by our group demonstrates that arylthiol-maleimide adducts and hydrogels (owing to the low pK_a of the aryl thiol) can undergo a retro Michael-type reaction and thiol-exchange in the presence of thiol-containing molecules (which leads to cross-link scission in the case of hydrogels), while alkylthiol-maleimide adducts and hydrogels exhibit limited activity in the retro reaction under the same conditions.^{62–65} More detailed investigations of the reactivity of various thiol compounds in retro Michael-type reaction and thiol-exchange are underway and will be the subject of future reports. Therefore, 4-arm PEG polymers functionalized with arylthiols (GSH-sensitive) or alkylthiols (GSH-insensitive) were utilized during hydrogel formation to selectively control network degradation (Scheme 1B). The liposome-cross-linked hybrid hydrogels (lipogels) were prepared subsequently by thiol-maleimide Michael-type addition between the thiol groups of the PEG polymers and the maleimide groups on the liposome surface, where the liposomes serve as structural elements (cross-links) within the polymer gel network (Scheme 2). As shown in the images, mixtures of solutions of the liposomes and thiol-functionalized PEG formed self-supporting hydrogels. Although it is possible that the 4-arm PEG-SH would also form disulfide-based crosslinks, the reaction kinetics of thiol oxidation (ca. $15.2 \text{ M}^{-1} \text{ s}^{-1}$)⁶⁸ are orders of magnitude slower than those of the Michael-type additions (ca. $1.3 \times 10^3 \text{ M}^{-1} \text{ s}^{-1}$),⁶⁹ so significant amounts of cross-linking due to disulfide bond formation were not expected. A key feature of the hydrogel design is that the thioether succinimide cross-links formed by the reaction of arylthiol moieties and

maleimide groups are degradable via a thiol-exchange reaction (enabled by retro-Michael-type addition reaction) in the presence of glutathione,^{62–65} which results in the degradation of the hydrogel to yield a viscous liquid (Scheme 2). We postulated that this would result in the release of the liposomes along with any encapsulated molecules in the hydrogels. These hydrogel compositions should therefore permit the triggered release of multiple compounds via passive diffusion from the hydrogel network and/or via thiol-triggered release of drug-containing liposomes.

Rheological Characterization

The ability of the maleimide-functionalized liposomes to form a percolated hydrogel network upon reaction with thiol-functionalized PEG was confirmed in a series of rheological experiments. Initial observations indicated that hydrogel formation required the presence of both maleimide-functionalized liposomes and 4-arm PEG-SH; the liposome and PEG polymer solutions alone remained low-viscosity liquids over the time scales at which gelation occurred (Scheme 2). Oscillatory time sweep and frequency sweep measurements were also performed to quantitatively monitor the in situ gelation and examine the stability of the three-dimensional cross-linked networks. Oscillatory frequency sweeps of the arylthiol-based hybrid hydrogels indicated the frequency dependence of both moduli, suggesting contributions from hydrophobic interactions between the liposomes and the PEG-arylthiol polymers (Supporting Information (SI), Figure S1),^{49,50} which complicated comparisons of mechanical properties between hydrogels of different polymer compositions. Therefore, in situ rheological results of the alkylthiol-based hydrogels are shown to simplify these comparisons. Rapid gelation of the materials (indicated here by the crossover point where G' (~0.40 Pa) becomes larger than G'' (~0.14 Pa), Figure S2) usually occurred within 5 min, which, owing to the rapid kinetics, excludes the possibility of gelation based on disulfide bonds and suggests that hydrogel formation is driven mainly by thiolmaleimide Michael-type addition reactions. Compared to other thiol-maleimide hydrogel systems,^{63,64,70,71} the gelation kinetics observed from the hybrid hydrogels were not as rapid, possibly due to steric hindrance and limited chemical accessibility of the maleimide groups on the liposome surface. The hydrogels were subsequently cured for 7 h to achieve maximum cross-linking. To further confirm that there was not significant cross-linking based on disulfide bonds, oscillatory time sweep experiments were performed on hydrogels comprising only 4-arm alkyl PEG-SH, where the lack of a significant increase in storage modulus suggested that disulfide cross-linking did not contribute significantly to the mechanical properties of the hydrogels (Figure S3).

Confirmation of the impact of the thiol-maleimide reaction on hydrogel properties was assessed by changing the ratio of maleimide groups (Mal) on the liposome surface to thiol groups (SH) on the PEG polymer. Initial experiments in which the liposome concentration was varied from 0.5 mM to 10 mM indicated that stable hydrogels could be formed reproducibly with liposome concentrations of at least 10 mM (data not shown). Owing to the ease with which the maleimide:thiol ratio could be reproducibly changed by varying thiol content (rather than by altering the amount of maleimide in the liposomes), liposome-containing precursor solutions were mixed with increasing fractions of alkylthiol PEG polymers (10 mM liposome solutions were mixed with 3, 6, and 12 wt % PEG,

corresponding to Mal:SH ratios of 1:1, 1:2, and 1:4 respectively). The storage and loss moduli (G' and G'' , respectively) of these hydrogels were measured as a function of frequency; representative data are presented in Figure 1A. The frequency independence of G' indicated the formation of a stable, cross-linked network with G' dominating in the entire frequency range of 0.1–100 rad/s. The data in Figure 1B more clearly highlight that the storage moduli of the liposome-cross-linked hydrogels increased from 1200 to 2500 Pa when the cross-linking ratios were varied from 1:1 (Mal:SH) to 1:2 (Mal:SH), a result in part due to the higher polymer concentration but also likely due to a reduction in the number of elastically inactive loops and unreacted chain ends when the stoichiometric ratio is 1:2. Other reports have shown that a 1:1 stoichiometric ratio rarely results in the highest storage modulus, owing to a reduced mobility of the cross-linker chains with increasing gel viscosity, which leads to incomplete reaction.^{72–74} However, when the amount of thiol was further increased (1:4 Mal:SH), the storage modulus of the hydrogels decreased to 1600 Pa despite the high concentration of polymer. The low degree of cross-linking at higher polymer concentration likely results from both steric hindrance and consumption of functional groups on the liposomes, thus reducing the extent of polymer bridging between liposomes.⁵² Owing to the more efficient cross-linking in the 1:2 Mal:SH hydrogel, this composition was employed in all further studies of the hydrogels. Taken together, these rheological results illustrate the relatively rapid formation of a stable, viscoelastic hydrogel network, indicative of network cross-linking based on the Michael-type addition (ca. $1.3 \times 10^3 \text{ M}^{-1} \text{ s}^{-1}$)⁶⁹ rather than disulfide formation (ca. $15.2 \text{ M}^{-1} \text{ s}^{-1}$).⁶⁸ Given the rapid gelation, mild preparation conditions, and biocompatibility of the thiol-maleimide cross-linking chemistry demonstrated by others in cell encapsulation^{75–77} and in vivo delivery,⁷¹ these hydrogels have significant potential for minimally invasive, direct injection applications.

Morphology of the Liposome-Cross-Linked Hydrogels

To visualize the liposomes in the hydrogel matrix, SEM was performed on the hybrid hydrogels after critical point drying. The representative SEM images in Figure 2 show that liposomes with a diameter of $105 \pm 25 \text{ nm}$ (calculated from analysis via ImageJ of over 200 particles and consistent with DLS characterization of liposomes liberated from the hydrogel (below)) are homogeneously distributed on the hydrogel surface; the apparently low number of liposomes detectable in these images is a result of the evaluation of strictly the surface of the hydrogels. The number of intact liposomes in the bulk of the hydrogel cannot be probed directly in the SEM experiment, but is indicated to be significantly greater than the density observed on the surface, given the robust mechanical properties of the liposome-cross-linked hydrogels (above) and the poor mechanical properties of a mixture of nonmaleimide liposomes and PEG-SH polymers (Figure S4). Although some ruptured liposomes can be observed in the SEM images above, possibly due to the drying process during sample preparation, the liposomes mainly retain their size and thus are indicated to remain intact throughout the cross-linking and degradation processes as indicated by the DLS characterization below. In contrast, no such nanostructure was observed in SEM images of a PEG hydrogel control lacking liposomes under the same conditions (Figure S5). These data are consistent with previous reports^{43,49,53} and confirm the structural integrity of the liposomes during the cross-linking reactions.

Hydrogel Stability

To verify the role of liposomes as cross-linkers in the polymer matrix, the liposome-cross-linked hydrogels were incubated with 10% Triton X-100, a nonionic detergent that solubilizes lipid bilayers.⁷⁸ Visual inspection and rheological characterization of the liposome-cross-linked hydrogels upon treatment with the Triton solution are shown in Figure 3. Images of the samples illustrate that opacity associated with the presence of liposome nanoparticles in the hydrogels was significantly reduced after incubation with Triton, suggesting the solubilization of liposomes within the network. The evolution of the storage modulus of the hydrogels during the incubation with Triton was also monitored via oscillatory rheology, where the initial modulus of the hydrogels prior to Triton addition was normalized to 1 to facilitate comparison. As expected, the Triton-treated hydrogels exhibited a rapid decrease in storage modulus to approximately 30% of its initial value within 3 h, whereas no significant change in normalized modulus was observed in the PEG hydrogel control under the same conditions. The rapid decrease in storage modulus of the hydrogels indicates a substantial decrease in the number of cross-links within the network as a result of the disruption of liposome bilayer structure by Triton X-100. Taken together, these results confirm that the maleimide-functionalized liposomes serve as cross-links within the hybrid hydrogels.

Thioether succinimide cross-links of maleimide-arylthiol hydrogels are known to undergo a retro Michael-type reaction and thiol-exchange, which leads to thiol-mediated network degradation.^{63–65} Although the kinetics of the retro-Michael addition and thiol exchange were independent of the use of glutathione disulfide (GSSG) or GSH as demonstrated in our previous report,⁶² suggesting that GSH in either of its forms will be competent for the thiol exchange, we specifically used GSH throughout this study (as opposed to other thiol-containing molecules such as GSSG and DTT) for hydrogel degradation due to the presence of GSH under physiologically/pathologically relevant conditions *in vivo*. GSH, a thiol-containing tripeptide localized in intracellular compartments,^{79,80} is found at elevated levels (ca. 0.5–10 mM) in various types of tumors (versus ca. 10 μ M in circulation), likely associated with increased cellular proliferation and metastatic activity.⁸¹ Therefore, the stability of these liposome-cross-linked hybrid hydrogels in the presence of GSH was evaluated by a series of mass loss studies in physiologically relevant buffer conditions (PBS) with GSH concentrations that are analogous to those of extracellular environments (ca. 10 μ M GSH) as well as intracellular compartments and carcinoma tissues (ca. 10 mM GSH).^{79,80} Figure 4 displays results from experiments in which the mass of the liposome-cross-linked hydrogels (synthesized from the PEG arylthiol (aryl lipogel) and from the alkyl PEG-SH (alkyl lipogel)) was monitored as a function of time. No significant loss of mass was observed for the aryl lipogel when it was incubated in PBS (~97% of the hydrogel remained intact at day 7), indicating the stability of such liposome-cross-linked hydrogels under physiologically relevant buffer conditions. Similarly, only slow and partial degradation of the aryl lipogel was observed for GSH concentrations of 10 μ M (with approximately 85% of the hydrogel remaining intact at day 7), demonstrating the stability of the hydrogels under conditions consistent with those in extracellular environments. At low concentrations of GSH, the hydrogel degradation rate is dependent on both the number of cross-links and the concentration of GSH. The degradation kinetics were thus calculated as second-order

much smaller nanoparticles with diameters of approximately 10 nm, consistent with the size of Triton-containing mixed micelles⁸³ and confirming the liposomal nature of the nanoparticles released from the hydrogel after treatment with GSH.

In Vitro Release of DOX from Liposome-Cross-Linked Hybrid Hydrogels

DOX, which is an anthracycline anticancer drug that inhibits the biosynthesis of bioactive macromolecules via interaction with DNA or RNA,^{84,85} was used as a model drug for in vitro release studies. Although the release of DOX has been widely explored in various delivery systems including liposomes,^{86,87} polymeric nanoparticles,^{88–92} and hydrogels,^{93–95} significant burst release is usually observed within 12–24 h in these systems. To evaluate the potential of our liposome-cross-linked hybrid hydrogels as a matrix for controlled delivery of DOX, drug-loaded liposome-cross-linked hydrogels were prepared by first encapsulating DOX into liposomes, followed by dissolution and cross-linking of the PEG-SH precursors in the suspension of these liposomes. The DOX released from these hydrogels will be subject to a combination of diffusion barriers: first the liposomal bilayer and then the polymer network, and the presence of the two barriers may minimize burst release and prolong release over an extended period of time. To test this, the release of DOX from liposome-cross-linked hydrogels synthesized from PEG arylthiol (aryl lipogel) and alkyl PEG-SH (alkyl lipogel), respectively, was monitored as a function of time at 37 °C in PBS containing 10 mM GSH (or in PBS alone), via measurement of the fluorescence intensity of the buffer in which the hydrogels were immersed (Figure 6).

As shown in Figure 6A, the aryl lipogel exhibited a diffuse boundary between the gel and the release buffer after incubation with GSH for 1 day, suggesting rapid GSH-mediated matrix degradation that is in agreement with the mass loss data above. In contrast, the aryl lipogel that was incubated with PBS showed a clear boundary between the gel and the buffer, indicating hydrogel stability and the lack of any significant release of DOX at early time points (indicated to be less than 7% via fluorimetry). The release profiles of DOX from these hydrogels are presented in Figure 6B. For the aryl lipogel incubated in 10 mM GSH, rapid, linear release of DOX was observed, with approximately 70% of the DOX released by day 6, commensurate with the time point at which significant hydrogel degradation occurred (visual inspection indicated the loss of hydrogel integrity and the presence of suspended particulate matter) and clearly different from the two control conditions. The release of DOX is not necessarily expected to correlate exactly with hydrogel degradation, as a significant fraction of the DOX is retained in the liposomes (demonstrated below). Modeling of the release data from the aryl lipogel in GSH according to the empirical Ritger–Peppas equation for non-Fickian transport^{96,97} yields a release rate constant of $4.55 \times 10^{-3} \text{ h}^{-1}$ (Figure S7A, eq 1 in the SI), indicating a degradation-based mechanism. For both the GSH-insensitive control (alkyl lipogel in GSH) and the GSH-lacking control (aryl lipogel in PBS), DOX was released in a relatively slow and sustained fashion, with a total of ca. 30–35% of DOX released in 10 days. The similarity in the DOX release between these two conditions is commensurate with their lack of significant matrix degradation in both cases (ca. 35% release for the alkyl lipogel in GSH vs ca. 30% release for the aryl lipogel in PBS at day 10, shown in Figure 6B).

The diffusion-controlled release of DOX from the two control lipogels lacking degradation was analyzed by fitting the data to the early time approximation of Fickian diffusion (Figure S7B, and eq 2 in the SI),^{40,98} which also yields similar rate constants of release for the two hydrogels ($2.88 \times 10^{-2} \text{ h}^{-1/2}$ for the alkyl lipogel in 10 mM GSH and $2.67 \times 10^{-2} \text{ h}^{-1/2}$ for the aryl lipogel in PBS). The goodness of the fit ($R^2 = 0.99$) indicated a diffusion-controlled mechanism of DOX release from the alkyl lipogel (GSH-insensitive) in 10 mM GSH solutions. In contrast, burst release (nearly 50% by day 1) was observed from a DOX-loaded PEG hydrogel control (PEG-arylthiol/PEG-maleimide) prepared without liposomes (regardless of GSH concentration, Figure S8), indicating that incorporation of liposomes within these hydrogel systems slows drug diffusion.

The key role of the liposomes in mediating the release of DOX was indicated by the observed additional burst release (ca. 30%) of DOX from aryl lipogels upon treatment with Triton X-100 (Figure S9). In addition, the sequestration of liberated, DOX-loaded liposomes in a dialysis cup (MWCO 3500) significantly depresses the amount of DOX that can be detected from GSH-containing buffer solutions surrounding the aryl lipogel, indicating that a significant fraction of the DOX released from the aryl lipogels (ca. 65% at day 6) is located in liberated liposomes (Figure S10). No such reduction in the amount of detected DOX is observed for the alkyl lipogel. These results in aggregate demonstrate that DOX release from the multicomponent hybrid hydrogels proceeds in a sustained manner without initial burst due to the liposome component and can be selectively triggered by thiol compounds that are known to be present in the tumor microenvironment.

Co-delivery of DOX and Cytochrome c

Combined and sequential delivery of two or multiple drugs with orthogonal and possibly synergistic mechanisms might not only improve therapeutic efficacy by affecting multiple disease targets, but also minimize side effects caused by high doses of a single toxic drug and delay the generation of drug resistance.^{11,99–101} As the liposomes constituted a structural component of the hybrid hydrogels, we anticipated that the multicomponent network would offer opportunities for dual encapsulation and differential release of multiple therapeutic cargo molecules. To examine the potential suitability of these hybrid hydrogels for such applications, cytochrome c, a small mitochondrial protein (~12 kDa) that can initiate an apoptotic cascade leading to programmed cell death upon cytoplasmic release,^{102–105} was chosen as a second therapeutic molecule. Dual encapsulation of DOX and cytochrome c in the hydrogels was carried out by dissolving cytochrome c along with the PEG-arylthiol polymers in DOX-loaded liposome suspensions. As a control, a solution of cytochrome c and PEG-arylthiol was evaluated after 1 h of incubation, with results demonstrating that the incubated cytochrome c electrophoresed almost identically to native cytochrome c during SDS-PAGE electrophoresis (Figure S11) and indicating that disulfide exchange between the protein and polymers was not significant within the time scale of the rapid cross-linking reaction.

In order to probe the differential release of both cargo molecules, the simultaneous release of both molecules from the hybrid hydrogels was monitored over time in 10 mM GSH solutions; results are presented in Figure 7. Consistent with our hypothesis, entirely different

release profiles for DOX and cytochrome c were observed from the liposome-cross-linked hybrid hydrogels (Figure 7A). The release profile of DOX demonstrates zero-order release kinetics, with approximately 70% release at day 6 (144 h), consistent with the observed release of DOX alone from the liposome-cross-linked hybrid hydrogels (Figure 6), and suggesting that DOX was released via erosion-mediated release of liposomes from the hydrogel surface in GSH-containing solutions. The release of cytochrome c, however, appears to be first-order, with almost 100% release within 6 days (144 h), consistent with the time scale of the GSH-induced degradation of the hydrogel (Figure 4). The surface erosion mechanism for the DOX, commensurate with the observation that the hydrogel decreased in size over time, may result from the localization of the arylthioether succinimide cross-links in the sterically hindered and relatively hydrophobic environment at the polymer–liposome interface, limiting the GSH exchange reactions within the matrix and resulting in a faster degradation rate on the hydrogel surface. Similar linear, zero-order release profiles of cargo loaded in the nanoparticles were also observed as a result of surface erosion in a hybrid hydrogel system employing drug-loaded poly-(ethylene glycol)-*block*-poly(lactic acid) nanoparticles as cross-linkers.⁵²

The release data for the DOX and the cytochrome c were modeled using the empirical Ritger–Peppas equation for non-Fickian transport^{96,97} (DOX, eq 1 in SI) and the late-time approximation equation derived from Fick's second law of diffusion^{106,107} (cytochrome c, eq 3 in the SI). The results from these fits indicate that the release rate constants k are $5.33 \times 10^{-3} \text{ h}^{-1}$ for DOX and $2.64 \times 10^{-2} \text{ h}^{-1}$ for cytochrome c, with the goodness of the fits indicating that the release of DOX from the hybrid hydrogels is dominated by a degradation-mediated release mechanism,⁵² while the release of cytochrome c from the hybrid hydrogels is governed by Fickian diffusion. Individual release of DOX and cytochrome c from separate hybrid hydrogels, measured in separate experiments and plotted together in Figure 7B, exhibited similar release kinetics compared to their counterparts when released simultaneously from a single gel, with release rate constants of $4.55 \times 10^{-3} \text{ h}^{-1}$ for DOX and $2.33 \times 10^{-2} \text{ h}^{-1}$ for cytochrome c. Statistical analysis of the release rate constants in both the simultaneous and individual release experiments shows that the release of cytochrome c is statistically the same in both cases. The release of DOX was suggested to be statistically slightly different ($p < 0.05$) in these experiments, which might be caused by slight batch-to-batch variations in DOX concentration in the liposomes.⁴⁹ Nevertheless, these results indicate that the release of the two therapeutic molecules is not affected substantially by their combined delivery; the sequential release of multiple therapeutic molecules is desirable for tailoring extended therapeutic regimens as well as for potentially promoting the transport and penetration of DOX-loaded liposomes to deep tissue of solid tumors through a tumor-priming mechanism.^{56,108,109} Similar differential release characteristics for multiple cargos have been observed in hydrogel nanocomposite drug delivery systems, where hydrophilic molecules encapsulated in the gel were released fairly rapidly while hydrophobic species encapsulated in the nanoparticles were released in a more sustained manner.^{52,110} Consistent with these reports, our results suggest that the liposome-cross-linked hybrid hydrogels containing both nanoparticle and polymer network domains can be exploited as a functional carrier for different therapeutics to be dually encapsulated and simultaneously released with differential profiles upon GSH-mediated degradation of the matrix.

to physiological and pathological states. Characterization of the hybrid hydrogels confirms the role of liposomes as cross-linkers and demonstrates the GSH-mediated network degradation and triggered release of encapsulated molecules. The multiple domains within the gel allow dual loading of therapeutic molecules that can be loaded in the liposomes and the bulk polymer network. Delivery experiments indicate that multiple therapeutic molecules encapsulated within the hydrogels can be released in a controlled and prolonged manner, with differential release profiles that are controlled by degradation-mediated release and Fickian diffusion. These results suggest the potential of these easily synthesized liposome-cross-linked hybrid hydrogels in advanced delivery applications.

Supplementary Material

Refer to Web version on PubMed Central for supplementary material.

Acknowledgments

This work was supported by the University of Delaware. The contents of the manuscript are the sole responsibility of the authors and do not necessarily reflect the official views of the University of Delaware. This project was also supported (instrumentation) by the Delaware COBRE program, with a grant from the National Institute of General Medical Sciences–NIGMS (1 P30 GM110758-01) from the National Institutes of Health. The authors also acknowledge Wenwen Liu for assistance with SEM imaging.

REFERENCES

1. Peer D, Karp JM, Hong S, Farokhzad OC, Margalit R, Langer R. Nanocarriers as an emerging platform for cancer therapy. *Nat. Nanotechnol.* 2007; 2(12):751–760. [PubMed: 18654426]
2. Davis ME, Chen Z, Shin DM. Nanoparticle therapeutics: an emerging treatment modality for cancer. *Nat. Rev. Drug Discovery.* 2008; 7(9):771–782. [PubMed: 18758474]
3. Hubbell JA, Chilkoti A. Nanomaterials for Drug Delivery. *Science.* 2012; 337(6092):303–305. [PubMed: 22822138]
4. Petros RA, DeSimone JM. Strategies in the design of nanoparticles for therapeutic applications. *Nat. Rev. Drug Discovery.* 2010; 9(8):615–627. [PubMed: 20616808]
5. Farokhzad OC, Langer R. Impact of Nanotechnology on Drug Delivery. *ACS Nano.* 2009; 3(1):16–20. [PubMed: 19206243]
6. Gao JH, Gu HW, Xu B. Multifunctional Magnetic Nanoparticles: Design, Synthesis, and Biomedical Applications. *Acc. Chem. Res.* 2009; 42(8):1097–1107. [PubMed: 19476332]
7. Ghosh P, Han G, De M, Kim CK, Rotello VM. Gold nanoparticles in delivery applications. *Adv. Drug Delivery Rev.* 2008; 60(11):1307–1315.
8. Pissuwan D, Niidome T, Cortie MB. The forthcoming applications of gold nanoparticles in drug and gene delivery systems. *J. Controlled Release.* 2011; 149(1):65–71.
9. Moon JJ, Suh H, Bershteyn A, Stephan MT, Liu HP, Huang B, Sohail M, Luo S, Um SH, Khant H, Goodwin JT, Ramos J, Chiu W, Irvine DJ. Interbilayer-crosslinked multilamellar vesicles as synthetic vaccines for potent humoral and cellular immune responses. *Nat. Mater.* 2011; 10(3):243–251. [PubMed: 21336265]
10. Joo KI, Xiao L, Liu SL, Liu YR, Lee CL, Conti PS, Wong MK, Li ZB, Wang P. Crosslinked multilamellar liposomes for controlled delivery of anticancer drugs. *Biomaterials.* 2013; 34(12):3098–3109. [PubMed: 23375392]
11. Liu YR, Fang JX, Kim YJ, Wong MK, Wang P. Codelivery of Doxorubicin and Paclitaxel by Cross-Linked Multilamellar Liposome Enables Synergistic Antitumor Activity. *Mol. Pharmaceutics.* 2014; 11(5):1651–1661.
12. Ding JX, Chen LH, Xiao CS, Chen L, Zhuang XL, Chen XS. Noncovalent interaction-assisted polymeric micelles for controlled drug delivery. *Chem. Commun.* 2014; 50(77):11274–11290.

13. Chen W, Meng FH, Cheng R, Deng C, Feijen J, Zhong ZY. Biodegradable glycopolymer-b-poly(epsilon-caprolactone) block copolymer micelles: versatile construction, tailored lactose functionality, and hepatoma-targeted drug delivery. *J. Mater. Chem. B.* 2015; 3(11):2308–2317.
14. Chen W, Meng FH, Cheng R, Deng C, Feijen J, Zhong Z. Facile construction of dual-bioresponsive biodegradable micelles with superior extracellular stability and activated intracellular drug release. *J. Controlled Release.* 2015; 210:125–133.
15. Azagarsamy MA, Alge DL, Radhakrishnan SJ, Tibbitt MW, Anseth KS. Photocontrolled Nanoparticles for On-Demand Release of Proteins. *Biomacromolecules.* 2012; 13(8):2219–2224. [PubMed: 22746981]
16. Liang Y, Kiick KL. Multifunctional lipid-coated polymer nanogels crosslinked by photo-triggered Michael-type addition. *Polym. Chem.* 2014; 5(5):1728–1736.
17. Heller DA, Levi Y, Pelet JM, Doloff JC, Wallas J, Pratt GW, Jiang S, Sahay G, Schroeder A, Schroeder JE, Chyan Y, Zurenko C, Querbes W, Manzano M, Kohane DS, Langer R, Anderson DG. Modular 'Click-in-Emulsion' Bone-Targeted Nanogels. *Adv. Mater.* 2013; 25(10):1449–1454. [PubMed: 23280931]
18. Shi JJ, Xiao ZY, Kamaly N, Farokhzad OC. Self-Assembled Targeted Nanoparticles: Evolution of Technologies and Bench to Bedside Translation. *Acc. Chem. Res.* 2011; 44(10):1123–1134. [PubMed: 21692448]
19. Byrne JD, Betancourt T, Brannon-Peppas L. Active targeting schemes for nanoparticle systems in cancer therapeutics. *Adv. Drug Delivery Rev.* 2008; 60(15):1615–1626.
20. Riehemann K, Schneider SW, Luger TA, Godin B, Ferrari M, Fuchs H. Nanomedicine-Challenge and Perspectives. *Angew. Chem., Int. Ed.* 2009; 48(5):872–897.
21. Barenholz Y. Doxil (R) - The first FDA-approved nano-drug: Lessons learned. *J. Controlled Release.* 2012; 160(2):117–134.
22. Allen TM, Cullis PR. Liposomal drug delivery systems: From concept to clinical applications. *Adv. Drug Delivery Rev.* 2013; 65(1):36–48.
23. Li YL, Rodrigues J, Tomas H. Injectable and biodegradable hydrogels: gelation, biodegradation and biomedical applications. *Chem. Soc Rev.* 2012; 41(6):2193–2221. [PubMed: 22116474]
24. Seliktar D. Designing Cell-Compatible Hydrogels for Biomedical Applications. *Science.* 2012; 336(6085):1124–1128. [PubMed: 22654050]
25. Censi R, Di Martino P, Vermonden T, Hennink WE. Hydrogels for protein delivery in tissue engineering. *J. Controlled Release.* 2012; 161(2):680–692.
26. Lin C-C, Anseth K. PEG Hydrogels for the Controlled Release of Biomolecules in Regenerative Medicine. *Pharm. Res.* 2009; 26(3):631–643. [PubMed: 19089601]
27. Vermonden T, Censi R, Hennink WE. Hydrogels for Protein Delivery. *Chem. Rev.* 2012; 112(5):2853–2888. [PubMed: 22360637]
28. Slaughter BV, Khurshid SS, Fisher OZ, Khademhosseini A, Peppas NA. Hydrogels in Regenerative Medicine. *Adv. Mater.* 2009; 21(32–33):3307–3329. [PubMed: 20882499]
29. Zhu J. Bioactive modification of poly(ethylene glycol) hydrogels for tissue engineering. *Biomaterials.* 2010; 31(17):4639–4656. [PubMed: 20303169]
30. Wallace DG, Cruise GM, Rhee WM, Schroeder JA, Prior JJ, Ju J, Maroney M, Duronio J, Ngo MH, Estridge T, Coker GC. A tissue sealant based on reactive multifunctional polyethylene glycol. *J. Biomed. Mater. Res.* 2001; 58(5):545–555. [PubMed: 11505430]
31. Wirostko B, Mann BK, Williams DL, Prestwich GD. Ophthalmic Uses of a Thiol-Modified Hyaluronan-Based Hydrogel. *Adv. Wound Care.* 2014; 3(11):708–716.
32. Gaharwar AK, Peppas NA, Khademhosseini A. Nanocomposite Hydrogels for Biomedical Applications. *Biotechnol. Bioeng.* 2014; 111(3):441–453. [PubMed: 24264728]
33. Thoniyot P, Tan MJ, Karim AA, Young DJ, Loh XJ. Nanoparticle-Hydrogel Composites: Concept, Design, and Applications of These Promising, Multi-Functional Materials. *Adv. Sci.* 2015; 2(1–2):140010.
34. Merino S, Martín C, Kostarelos K, Prato M, Vázquez E. Nanocomposite Hydrogels: 3D Polymer-Nanoparticle Synergies for On-Demand Drug Delivery. *ACS Nano.* 2015; 9(5):4686–4697. [PubMed: 25938172]

35. Wang C, Flynn NT, Langer R. Controlled structure and properties of thermoresponsive nanoparticle-hydrogel composites. *Adv. Mater.* 2004; 16(13):1074–1079.
36. Shin SR, Jung SM, Zalabany M, Kim K, Zorlutuna P, Kim SB, Nikkiah M, Khabiry M, Azize M, Kong J, Wan KT, Palacios T, Dokmeci MR, Bae H, Tang XW, Khademhosseini A. Carbon-Nanotube-Embedded Hydrogel Sheets for Engineering Cardiac Constructs and Bioactuators. *ACS Nano.* 2013; 7(3):2369–2380. [PubMed: 23363247]
37. Chung YI, Ahn KM, Jeon SH, Lee SY, Lee JH, Tae G. Enhanced bone regeneration with BMP-2 loaded functional nanoparticle-hydrogel complex. *J. Controlled Release.* 2007; 121(1–2):91–99.
38. Gao WW, Hu CMJ, Fang RH, Zhang LF. Liposome-like nanostructures for drug delivery. *J. Mater. Chem. B.* 2013; 1(48):6569–6585.
39. Popescu MT, Mourtas S, Pampalakis G, Antimisariis SG, Tsitsilianis C. pH-Responsive Hydrogel/Liposome Soft Nanocomposites For Tuning Drug Release. *Biomacromolecules.* 2011; 12(8): 3023–3030. [PubMed: 21728314]
40. Gao WW, Vecchio D, Li JM, Zhu JY, Zhang QZ, Fu V, Li JY, Thamphiwatana S, Lu DN, Zhang LF. Hydrogel Containing Nanoparticle-Stabilized Liposomes for Topical Antimicrobial Delivery. *ACS Nano.* 2014; 8(3):2900–2907. [PubMed: 24483239]
41. Widjaja LK, Bora M, Chan PNP, Lipik V, Wong TTL, Venkatraman SS. Hyaluronic acid-based nanocomposite hydrogels for ocular drug delivery applications. *J. Biomed. Mater. Res., Part A.* 2014; 102(9):3056–3065.
42. Lopez-Noriega A, Hastings CL, Ozbakir B, O'Donnell KE, O'Brien FJ, Storm G, Hennink WE, Duffy GP, Ruiz-Hernandez E. Hyperthermia-Induced Drug Delivery from Thermo-sensitive Liposomes Encapsulated in an Injectable Hydrogel for Local Chemotherapy. *Adv. Healthcare Mater.* 2014; 3(6):854–859.
43. Wickremasinghe NC, Kumar VA, Hartgerink JD. Two-Step Self-Assembly of Liposome-Multidomain Peptide Nanofiber Hydrogel for Time-Controlled Release. *Biomacromolecules.* 2014; 15(10):3587–3595. [PubMed: 25308335]
44. Wickremasinghe NC, Kumar VA, Shi S, Hartgerink JD. Controlled Angiogenesis in Peptide Nanofiber Composite Hydrogels. *ACS Biomater. Sci. Eng.* 2015; 1(9):845–854. [PubMed: 26925462]
45. Souza GR, Christianson DR, Staquicini FI, Ozawa MG, Snyder EY, Sidman RL, Miller JH, Arap W, Pasqualini R. Networks of gold nanoparticles and bacteriophage as biological sensors and cell-targeting agents. *Proc. Natl. Acad. Sci. U. S. A.* 2006; (103)(5):1215–1220. [PubMed: 16434473]
46. Castaneda L, Valle J, Yang N, Pluskat S, Slowinska K. Collagen Cross-Linking with Au Nanoparticles. *Biomacromolecules.* 2008; 9(12):3383–3388. [PubMed: 18959440]
47. Skardal A, Zhang JX, McCoard L, Oottamasathien S, Prestwich GD. Dynamically Crosslinked Gold Nanoparticle - Hyaluronan Hydrogels. *Adv. Mater.* 2010; 22(42):4736–4740. [PubMed: 20730818]
48. Xiao LX, Tong ZX, Chen YC, Pochan DJ, Sabanayagam CR, Jia XQ. Hyaluronic Acid-Based Hydrogels Containing Covalently Integrated Drug Depots: Implication for Controlling Inflammation in Mechanically Stressed Tissues. *Biomacromolecules.* 2013; 14(11):3808–3819. [PubMed: 24093583]
49. Lee JH, Oh H, Baxa U, Raghavan SR, Blumenthal R. Biopolymer-Connected Liposome Networks as Injectable Biomaterials Capable of Sustained Local Drug Delivery. *Biomacromolecules.* 2012; 13(10):3388–3394. [PubMed: 22970880]
50. Chen YJ, Javvaji V, MacIntire IC, Raghavan SR. Gelation of Vesicles and Nanoparticles Using Water-Soluble Hydrophobically Modified Chitosan. *Langmuir.* 2013; 29(49):15302–15308. [PubMed: 24279281]
51. Javvaji V, Dowling MB, Oh H, White IM, Raghavan SR. Reversible gelation of cells using self-assembling hydrophobically-modified biopolymers: towards self-assembly of tissue. *Biomater. Sci.* 2014; 2(7):1016–1023.
52. Appel EA, Tibbitt MW, Webber MJ, Mattix BA, Veiseh O, Langer R. Self-assembled hydrogels utilizing polymer-nanoparticle interactions. *Nat. Commun.* 2015; 6:6295. [PubMed: 25695516]

53. Sekine Y, Moritani Y, Ikeda-Fukazawa T, Sasaki Y, Akiyoshi K. A Hybrid Hydrogel Biomaterial by Nanogel Engineering: Bottom-Up Design with Nanogel and Liposome Building Blocks to Develop a Multidrug Delivery System. *Adv. Healthcare Mater.* 2012; 1(6):722–728.
54. Hashimoto Y, Mukai S, Sawada S, Sasaki Y, Akiyoshi K. Nanogel tectonic porous gel loading biologics, nanocarriers, and cells for advanced scaffold. *Biomaterials.* 2015; 37:107–115. [PubMed: 25453324]
55. Journe F, Chaboteaux C, Laurent G, Body JJ. Sequence-dependent synergistic effects of ibandronate in combination with antiestrogens on growth inhibition of estrogen receptor-positive breast cancer cells. *Bone.* 2006; 38(3):S52–S53.
56. Hu CM, Aryal S, Zhang L. Nanoparticle-assisted combination therapies for effective cancer treatment. *Ther. Delivery.* 2010; 1(2):323–334.
57. Zhang LM, Lu ZX, Zhao QH, Huang J, Shen H, Zhang ZJ. Enhanced Chemotherapy Efficacy by Sequential Delivery of siRNA and Anticancer Drugs Using PEI-Grafted Graphene Oxide. *Small.* 2011; 7(4):460–464. [PubMed: 21360803]
58. Godsey ME, Suryaprakash S, Leong KW. Materials innovation for co-delivery of diverse therapeutic cargos. *RSC Adv.* 2013; 3(47):24794–24811. [PubMed: 24818000]
59. Yilgor P, Tuzlakoglu K, Reis RL, Hasirci N, Hasirci V. Incorporation of a sequential BMP-2/BMP-7 delivery system into chitosan-based scaffolds for bone tissue engineering. *Biomaterials.* 2009; 30(21):3551–3559. [PubMed: 19361857]
60. Chen FM, Zhang M, Wu ZF. Toward delivery of multiple growth factors in tissue engineering. *Biomaterials.* 2010; 31(24):6279–6308. [PubMed: 20493521]
61. Ilg P. Stimuli-responsive hydrogels cross-linked by magnetic nanoparticles. *Soft Matter.* 2013; 9(13):3465–3468.
62. Baldwin AD, Kiick KL. Tunable Degradation of Maleimide-Thiol Adducts in Reducing Environments. *Bioconjugate Chem.* 2011; 22(10):1946–1953.
63. Baldwin AD, Kiick KL. Reversible maleimide-thiol adducts yield glutathione-sensitive poly(ethylene glycol)-heparin hydrogels. *Polym. Chem.* 2013; 4(1):133–143. [PubMed: 23766781]
64. Kharkar PM, Kloxin AM, Kiick KL. Dually degradable click hydrogels for controlled degradation and protein release. *J. Mater. Chem. B.* 2014; 2(34):5511–5521.
65. Kharkar PM, Kiick KL, Kloxin AM. Design of thiol- and light-sensitive degradable hydrogels using Michael-type addition reactions. *Polym. Chem.* 2015; 6(31):5565–5574. [PubMed: 26284125]
66. Lyon RP, Setter JR, Bovee TD, Doronina SO, Hunter JH, Anderson ME, Balasubramanian CL, Duniho SM, Leiske CI, Li F, Senter PD. Self-hydrolyzing maleimides improve the stability and pharmacological properties of antibody-drug conjugates. *Nat. Biotechnol.* 2014; 32(10):1059–1062. [PubMed: 25194818]
67. Elbert DL, Pratt AB, Lutolf MP, Halstenberg S, Hubbell JA. Protein delivery from materials formed by self-selective conjugate addition reactions. *J. Controlled Release.* 2001; 76(1–2):11–25.
68. Luo DY, Smith SW, Anderson BD. Kinetics and mechanism of the reaction of cysteine and hydrogen peroxide in aqueous solution. *J. Pharm. Sci.* 2005; 94(2):304–316. [PubMed: 15570599]
69. Fontaine SD, Reid R, Robinson L, Ashley GW, Santi DV. Long-Term Stabilization of Maleimide-Thiol Conjugates. *Bioconjugate Chem.* 2015; 26(1):145–152.
70. Nie T, Baldwin A, Yamaguchi N, Kiick KL. Production of heparin-functionalized hydrogels for the development of responsive and controlled growth factor delivery systems. *J. Controlled Release.* 2007; 122(3):287–296.
71. Baldwin AD, Robinson KG, Militar JL, Derby CD, Kiick KL, Akins RE. In situ crosslinkable heparin-containing poly(ethylene glycol) hydrogels for sustained anticoagulant release. *J. Biomed. Mater. Res., Part A.* 2012; 100A(8):2106–2118.
72. Lutolf MP, Hubbell JA. Synthesis and Physicochemical Characterization of End-Linked Poly(ethylene glycol)-co-peptide Hydrogels Formed by Michael-Type Addition. *Biomacromolecules.* 2003; 4(3):713–722. [PubMed: 12741789]
73. Paradee N, Sirivat A, Niamlang S, Prissanaroon-Oujai W. Effects of crosslinking ratio, model drugs, and electric field strength on electrically controlled release for alginate-based hydrogel. *J. Mater. Sci.: Mater. Med.* 2012; 23(4):999–1010. [PubMed: 22354328]

74. Pakulska MM, Vulic K, Tam RY, Shoichet MS. Hybrid Crosslinked Methylcellulose Hydrogel: A Predictable and Tunable Platform for Local Drug Delivery. *Adv. Mater.* 2015; 27(34):5002–5008. [PubMed: 26184559]
75. Phelps EA, Enemchukwu NO, Fiore VF, Sy JC, Murthy N, Sulchek TA, Barker TH, Garcia AJ. Maleimide Cross-Linked Bioactive PEG Hydrogel Exhibits Improved Reaction Kinetics and Cross-Linking for Cell Encapsulation and In Situ Delivery. *Adv. Mater.* 2012; 24(1):64–70. [PubMed: 22174081]
76. Tsurkan MV, Chwalek K, Prokoph S, Zieris A, Levental KR, Freudenberg U, Werner C. Defined Polymer-Peptide Conjugates to Form Cell-Instructive starPEG-Heparin Matrices In Situ. *Adv. Mater.* 2013; 25(18):2606–2610. [PubMed: 23576312]
77. Chwalek K, Tsurkan MV, Freudenberg U, Werner C. Glycosaminoglycan-based hydrogels to modulate heterocellular communication in in vitro angiogenesis models. *Sci. Rep.* 2014; 4:4414. [PubMed: 24643064]
78. Mattei B, Franca ADC, Riske KA. Solubilization of Binary Lipid Mixtures by the Detergent Triton X-100: The Role of Cholesterol. *Langmuir.* 2015; 31(1):378–386. [PubMed: 25474726]
79. Meng FH, Hennink WE, Zhong Z. Reduction-sensitive polymers and bioconjugates for biomedical applications. *Biomaterials.* 2009; 30(12):2180–2198. [PubMed: 19200596]
80. Cheng R, Feng F, Meng F, Deng C, Feijen J, Zhong Z. Glutathione-responsive nano-vehicles as a promising platform for targeted intracellular drug and gene delivery. *J. Controlled Release.* 2011; 152(1):2–12.
81. Traverso N, Ricciarelli R, Nitti M, Marengo B, Furfaro AL, Pronzato MA, Marinari UM, Domenicotti C. Role of Glutathione in Cancer Progression and Chemoresistance. *Oxid. Med. Cell. Longevity.* 2013; 2013:1.
82. Ghosh K, Shu XZ, Mou R, Lombardi J, Prestwich GD, Rafailovich MH, Clark RAF. Rheological characterization of in situ cross-linkable hyaluronan hydrogels. *Biomacromolecules.* 2005; 6(5): 2857–2865. [PubMed: 16153128]
83. Kazakov S, Kaholek M, Teraoka I, Levon K. UV-induced gelation on nanometer scale using liposome reactor. *Macromolecules.* 2002; 35(5):1911–1920.
84. Fornari FA, Randolph JK, Yalowich JC, Ritke MK, Gewirtz DA. Interference by Doxorubicin with DNA Unwinding in MCF-7 Breast-Tumor Cells. *Mol. Pharmacol.* 1994; 45(4):649–656. [PubMed: 8183243]
85. Tacar O, Sriamornsak P, Dass CR. Doxorubicin: an update on anticancer molecular action, toxicity and novel drug delivery systems. *J. Pharm. Pharmacol.* 2013; 65(2):157–170. [PubMed: 23278683]
86. Wang ZH, Yu Y, Dai WB, Lu JK, Cui JR, Wu HN, Yuan L, Zhang H, Wang XQ, Wang JC, Zhang X, Zhang Q. The use of a tumor metastasis targeting peptide to deliver doxorubicin-containing liposomes to highly metastatic cancer. *Biomaterials.* 2012; 33(33):8451–8460. [PubMed: 22940213]
87. Zhao Y, Alakhova DY, Kim JO, Bronich TK, Kabanov AV. A simple way to enhance Doxil (R) therapy: Drug release from liposomes at the tumor site by amphiphilic block copolymer. *J. Controlled Release.* 2013; 168(1):61–69.
88. Missirlis D, Kawamura R, Tirelli N, Hubbell JA. Doxorubicin encapsulation and diffusional release from stable, polymeric, hydrogel nanoparticles. *Eur. J. Pharm. Sci.* 2006; 29(2):120–129. [PubMed: 16904301]
89. Ding JX, Shi FH, Xiao CS, Lin L, Chen L, He CL, Zhuang XL, Chen XS. One-step preparation of reduction-responsive poly(ethylene glycol)-poly (amino acid)s nanogels as efficient intracellular drug delivery platforms. *Polym. Chem.* 2011; 2(12):2857–2864.
90. Zhong YN, Yang WJ, Sun HL, Cheng R, Meng FH, Deng C, Zhong ZY. Ligand-Directed Reduction-Sensitive Shell-Sheddable Biodegradable Micelles Actively Deliver Doxorubicin into the Nuclei of Target Cancer Cells. *Biomacromolecules.* 2013; 14(10):3723–3730. [PubMed: 23998942]
91. Chen W, Zou Y, Meng FH, Cheng R, Deng C, Feijen J, Zhong ZY. Glyco-Nanoparticles with Sheddable Saccharide Shells: A Unique and Potent Platform for Hepatoma-Targeting Delivery of Anticancer Drugs. *Biomacromolecules.* 2014; 15(3):900–907. [PubMed: 24460130]

92. Loh XJ, del Barrio J, Toh PPC, Lee TC, Jiao DZ, Rauwald U, Appel EA, Scherman OA. Triply Triggered Doxorubicin Release From Supramolecular Nanocontainers. *Biomacromolecules*. 2012; 13(1):84–91. [PubMed: 22148638]
93. Kuang HH, He HY, Zhang ZY, Qi YX, Xie ZG, Jing XB, Huang YB. Injectable and biodegradable supramolecular hydrogels formed by nucleobase-terminated poly(ethylene oxide)s and alpha-cyclodextrin. *J. Mater. Chem. B*. 2014; 2(6):659–667.
94. Shi JB, Guobao W, Chen HL, Zhong W, Qiu XZ, Xing MMQ. Schiff based injectable hydrogel for in situ pH-triggered delivery of doxorubicin for breast tumor treatment. *Polym. Chem*. 2014; 5(21):6180–6189.
95. Xiong L, Luo Q, Wang Y, Li X, Shen Z, Zhu W. An injectable drug-loaded hydrogel based on a supramolecular polymeric prodrug. *Chem. Commun*. 2015; 51(78):14644–14647.
96. Serra L, Domenech J, Peppas NA. Drug transport mechanisms and release kinetics from molecularly designed poly-(acrylic acid-g-ethylene glycol) hydrogels. *Biomaterials*. 2006; 27(31):5440–5451. [PubMed: 16828864]
97. Siepmann J, Peppas NA. Modeling of drug release from delivery systems based on hydroxypropyl methylcellulose (HPMC). *Adv. Drug Delivery Rev*. 2012; 64:163–174.
98. Siepmann J, Peppas NA. Higuchi equation: Derivation, applications, use and misuse. *Int. J. Pharm*. 2011; 418(1):6–12. [PubMed: 21458553]
99. Li D, Li YB, Xing HB, Guo JL, Ping Y, Tang GP. Synergistic Enhancement of Lung Cancer Therapy Through Nano-carrier-Mediated Sequential Delivery of Superantigen and Tyrosin Kinase Inhibitor. *Adv. Funct. Mater*. 2014; 24(35):5482–5492.
100. Yoon HY, Son S, Lee SJ, You DG, Yhee JY, Park JH, Swierczewska M, Lee S, Kwon IC, Kim SH, Kim K, Pomper MG. Glycol chitosan nanoparticles as specialized cancer therapeutic vehicles: Sequential delivery of doxorubicin and Bcl-2 siRNA. *Sci. Rep*. 2014; 4:6878. [PubMed: 25363213]
101. Wang WW, Song HJ, Zhang J, Li P, Li C, Wang C, Kong DL, Zhao Q. An injectable, thermosensitive and multicompartment hydrogel for simultaneous encapsulation and independent release of a drug cocktail as an effective combination therapy platform. *J. Controlled Release*. 2015; 203:57–66.
102. Barczyk K, Kreuter M, Pryjma J, Booy EP, Maddika S, Ghavami S, Berdel WE, Roth J, Los M. Serum cytochrome c indicates in vivo apoptosis and can serve as a prognostic marker during cancer therapy. *Int. J. Cancer*. 2005; 116(2):167–173. [PubMed: 15800951]
103. Santra S, Kaittanis C, Perez JM. Cytochrome c Encapsulating Theranostic Nanoparticles: A Novel Bifunctional System for Targeted Delivery of Therapeutic Membrane-Impermeable Proteins to Tumors and Imaging of Cancer Therapy. *Mol. Pharmaceutics*. 2010; 7(4):1209–1222.
104. Kim SK, Foote MB, Huang L. The targeted intracellular delivery of cytochrome C protein to tumors using lipid-apolipoprotein nanoparticles. *Biomaterials*. 2012; 33(15):3959–3966. [PubMed: 22365810]
105. Tang YX, Teng ZG, Liu Y, Tian Y, Sun J, Wang SJ, Wang CY, Wang JD, Lu GM. Cytochrome C capped mesoporous silica nanocarriers for pH-sensitive and sustained drug release. *J. Mater. Chem. B*. 2014; 2(27):4356–4362.
106. Siepmann J, Siepmann F. Mathematical modeling of drug delivery. *Int. J. Pharm*. 2008; 364(2):328–343. [PubMed: 18822362]
107. Fu Y, Kao WJ. Drug release kinetics and transport mechanisms of non-degradable and degradable polymeric delivery systems. *Expert Opin. Drug Delivery*. 2010; 7(4):429–444.
108. Lu D, Wientjes MG, Lu Z, Au JLS. Tumor priming enhances delivery and efficacy of nanomedicines. *J. Pharmacol. Exp. Ther*. 2007; 322(1):80–88. [PubMed: 17420296]
109. Lu Z, Tsai M, Lu D, Wang J, Wientjes MG, Au JLS. Tumor-Penetrating Microparticles for Intraperitoneal Therapy of Ovarian Cancer. *J. Pharmacol. Exp. Ther*. 2008; 327(3):673–682. [PubMed: 18780831]
110. Baumann MD, Kang CE, Stanwick JC, Wang YF, Kim H, Lapitsky Y, Shoichet MS. An injectable drug delivery platform for sustained combination therapy. *J. Controlled Release*. 2009; 138(3):205–213.

111. Sasisekharan R, Shriver Z, Venkataraman G, Narayanasami U. Roles of heparan-sulphate glycosaminoglycans in cancer. *Nat. Rev. Cancer.* 2002; 2(7):521–528. [PubMed: 12094238]
112. Liang Y, Kiick KL. Heparin-functionalized polymeric biomaterials in tissue engineering and drug delivery applications. *Acta Biomater.* 2014; 10(4):1588–1600. [PubMed: 23911941]
113. Herrera-Gayol A, Jothy S. Effect of Hyaluronan on Xenotransplanted Breast Cancer. *Exp. Mol. Pathol.* 2002; 72(3):179–185. [PubMed: 12009781]
114. Tan S, Li X, Guo Y, Zhang Z. Lipid-enveloped hybrid nanoparticles for drug delivery. *Nanoscale.* 2013; 5(3):860–872. [PubMed: 23292080]
115. Krishnamurthy S, Vaiyapuri R, Zhang L, Chan JM. Lipid-coated polymeric nanoparticles for cancer drug delivery. *Biomater. Sci.* 2015; 3(7):923–936. [PubMed: 26221931]
116. Raemdonck K, Braeckmans K, Demeester J, De Smedt SC. Merging the best of both worlds: hybrid lipid-enveloped matrix nanocomposites in drug delivery. *Chem. Soc. Rev.* 2014; 43(1): 444–472. [PubMed: 24100581]

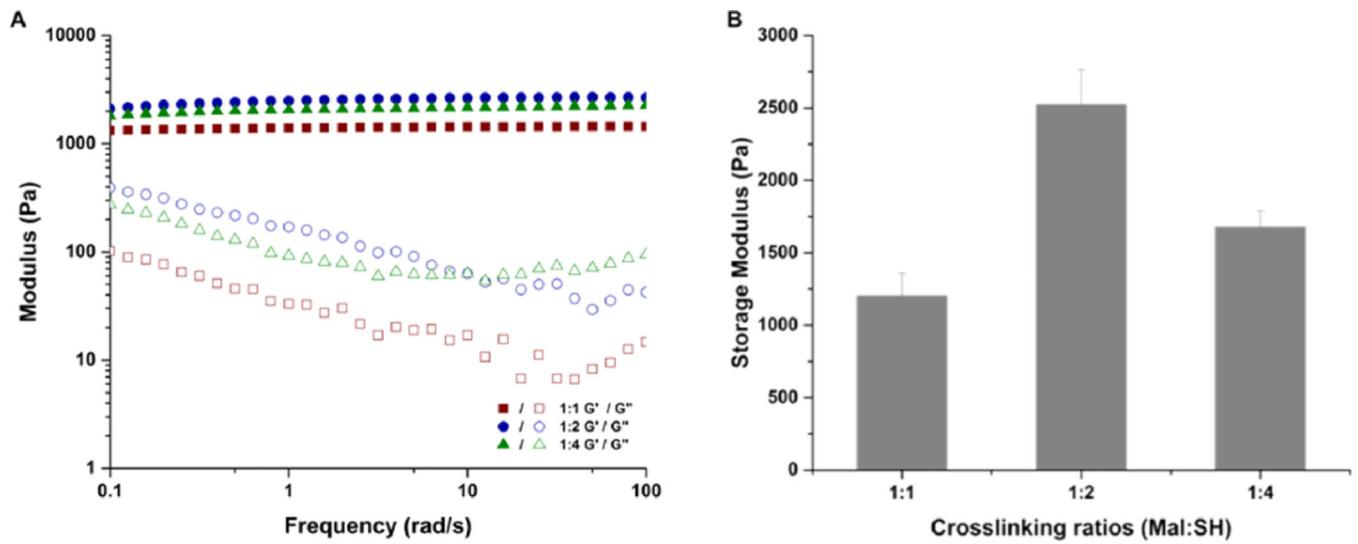


Figure 1. Rheological characterization of liposome-cross-linked hybrid hydrogels at various cross-linking ratios (1:1, 1:2, and 1:4 Mal:SH ratios). (A) Oscillatory frequency sweep of the hydrogels from 0.1 to 100 rad/s at 1% strain amplitude. (B) Summary of storage moduli (G') of hydrogels prepared at different cross-linking ratios.

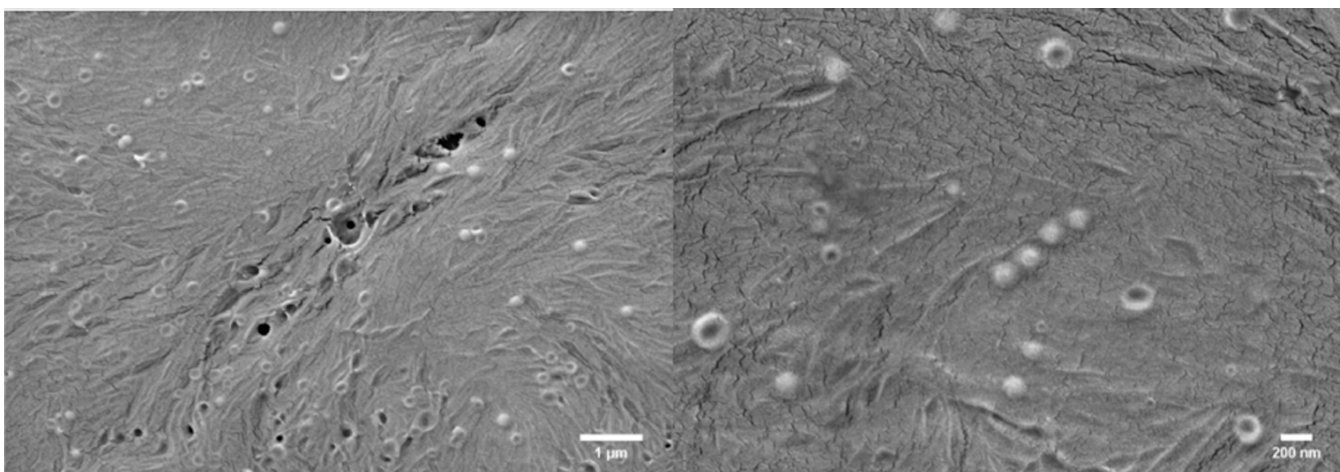


Figure 2. SEM images of the liposome-cross-linked hybrid hydrogels after critical point drying. The average diameter of the liposomes embedded in the gel is 105 ± 25 nm, as analyzed by ImageJ.

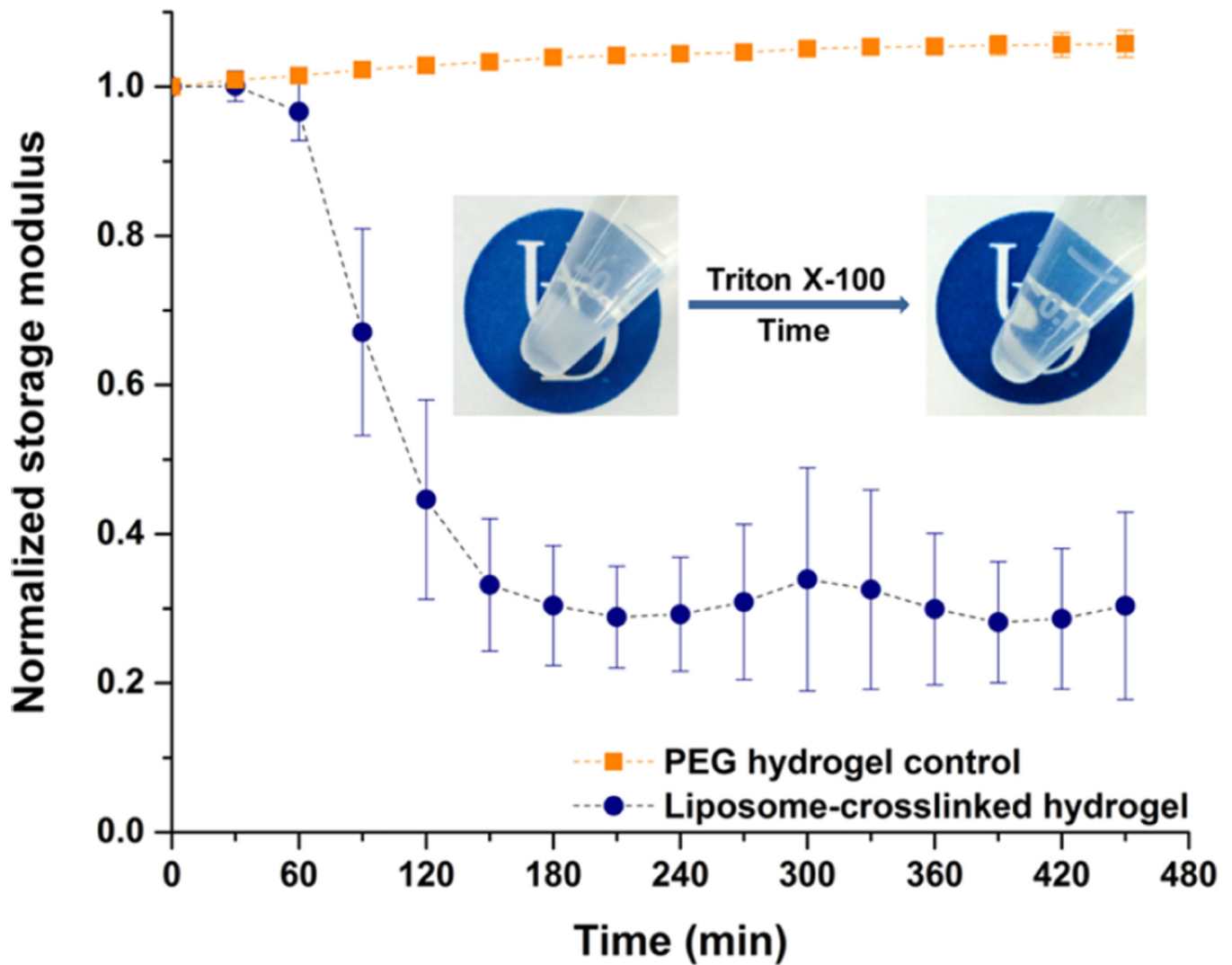


Figure 3. Evolution of storage modulus of the liposome-cross-linked hydrogel, as well as a PEG hydrogel control, when incubated with 10% Triton X-100 in water at 37 °C, as monitored by oscillatory rheology. Mean and standard deviation (SD) are shown ($n = 3$). Inset: visual inspection of the liposome-cross-linked hydrogel immersed in 10% Triton X-100 at 37 °C over time. Both hydrogel images were taken with 10% Triton X-100 in the supernatant to mimic the conditions in the rheological measurements and to provide parallel comparisons. The UD logos are used with permission from the University of Delaware.

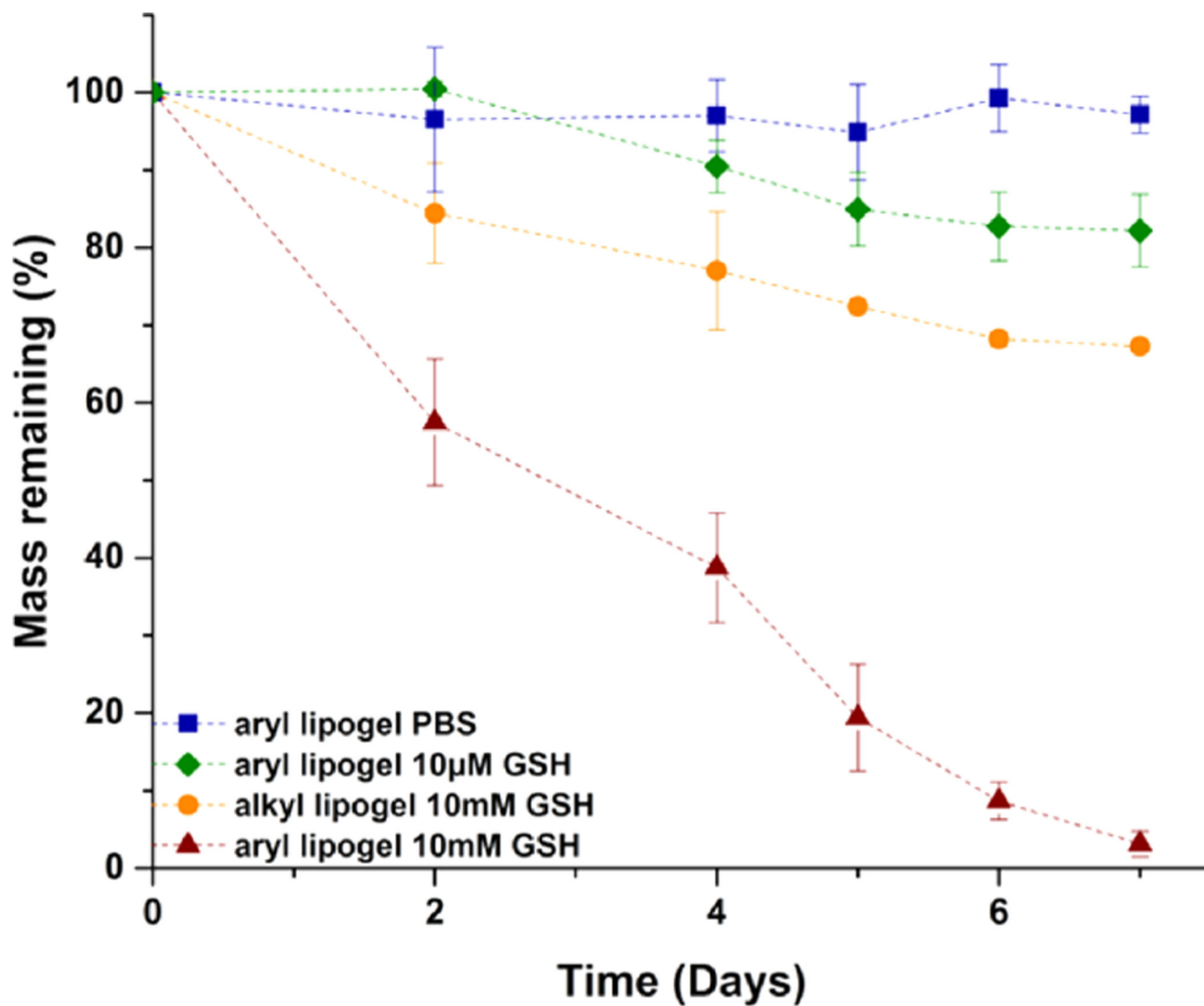


Figure 4. Mass loss studies of the liposome-cross-linked hybrid hydrogels incubated with PBS and GSH of various concentrations at 37 °C after initial equilibrium swelling in PBS for 24 h. Mean and SD are shown ($n = 3$).

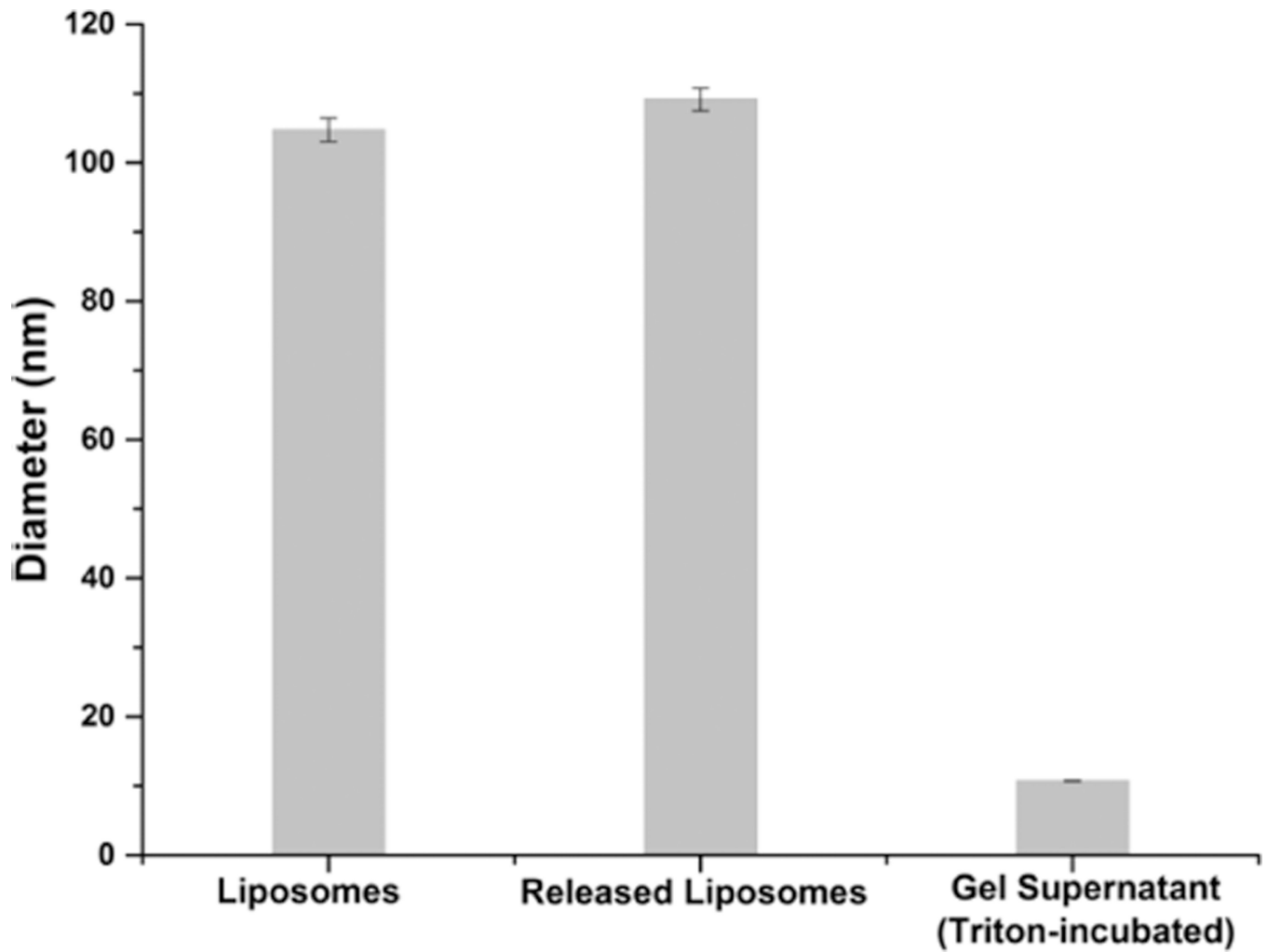


Figure 5. Hydrodynamic diameter of liposomes prior to hydrogel formation, released liposomes after complete network degradation in 10 mM GSH, and any particles in the gel supernatant after incubation with Triton X-100 at 37 °C, as determined by DLS.

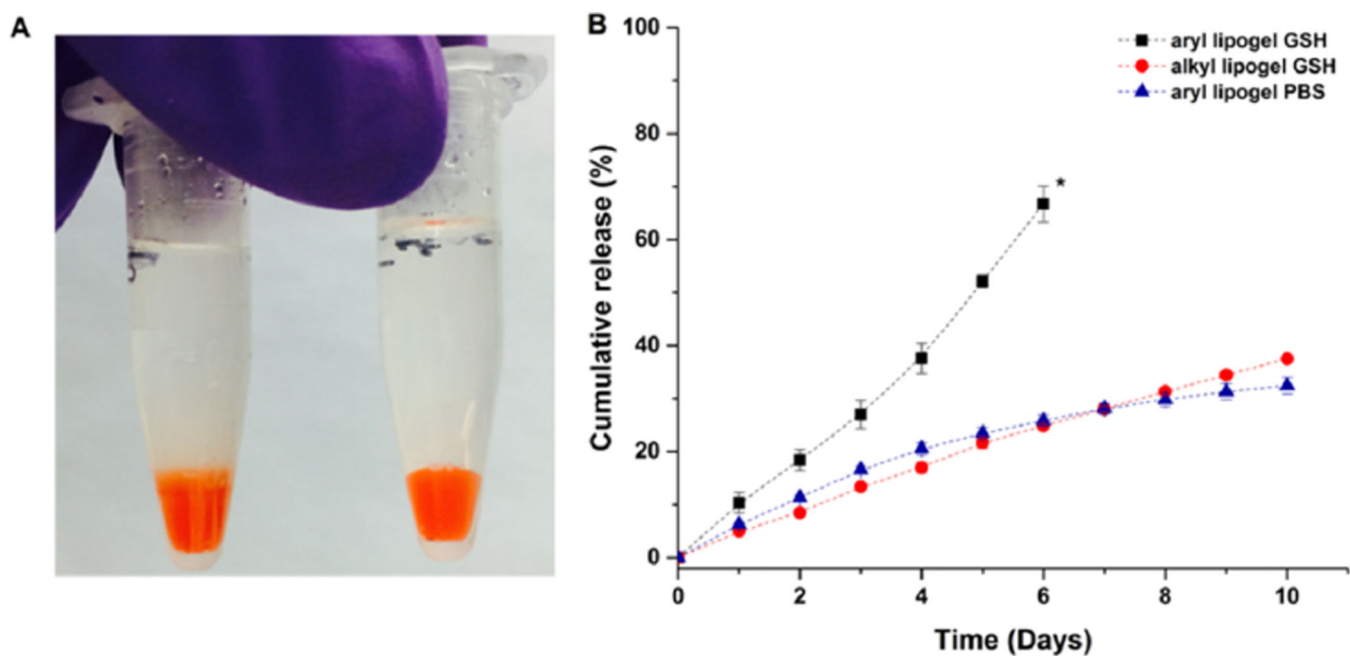


Figure 6.

In vitro release of DOX from the liposome-cross-linked hydrogels at 37 °C as assessed via visual inspection and fluorimetry. (A) Image of DOX-loaded liposome-cross-linked hydrogels incubated in 10 mM GSH (left, diffuse boundary observed) and PBS (right, clear boundary maintained) solutions on day 1. (B) Cumulative release profiles of DOX from liposome-cross-linked hydrogels in 10 mM GSH or in PBS solutions. * indicates the time point where ~90% hydrogel dissolution was observed. Mean and SD are shown ($n = 3$).

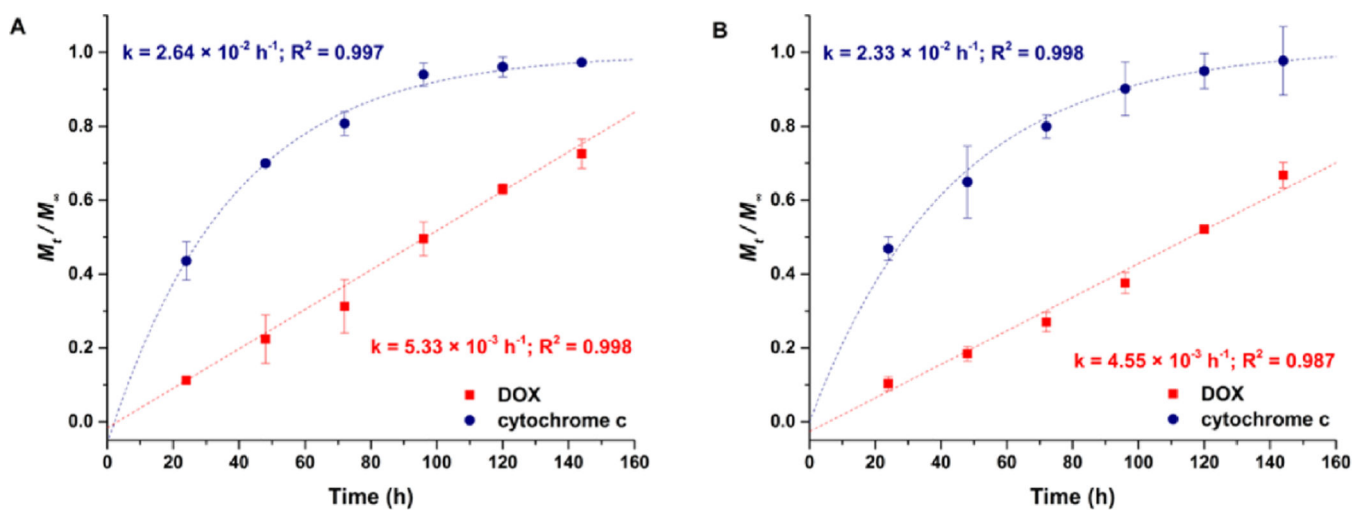
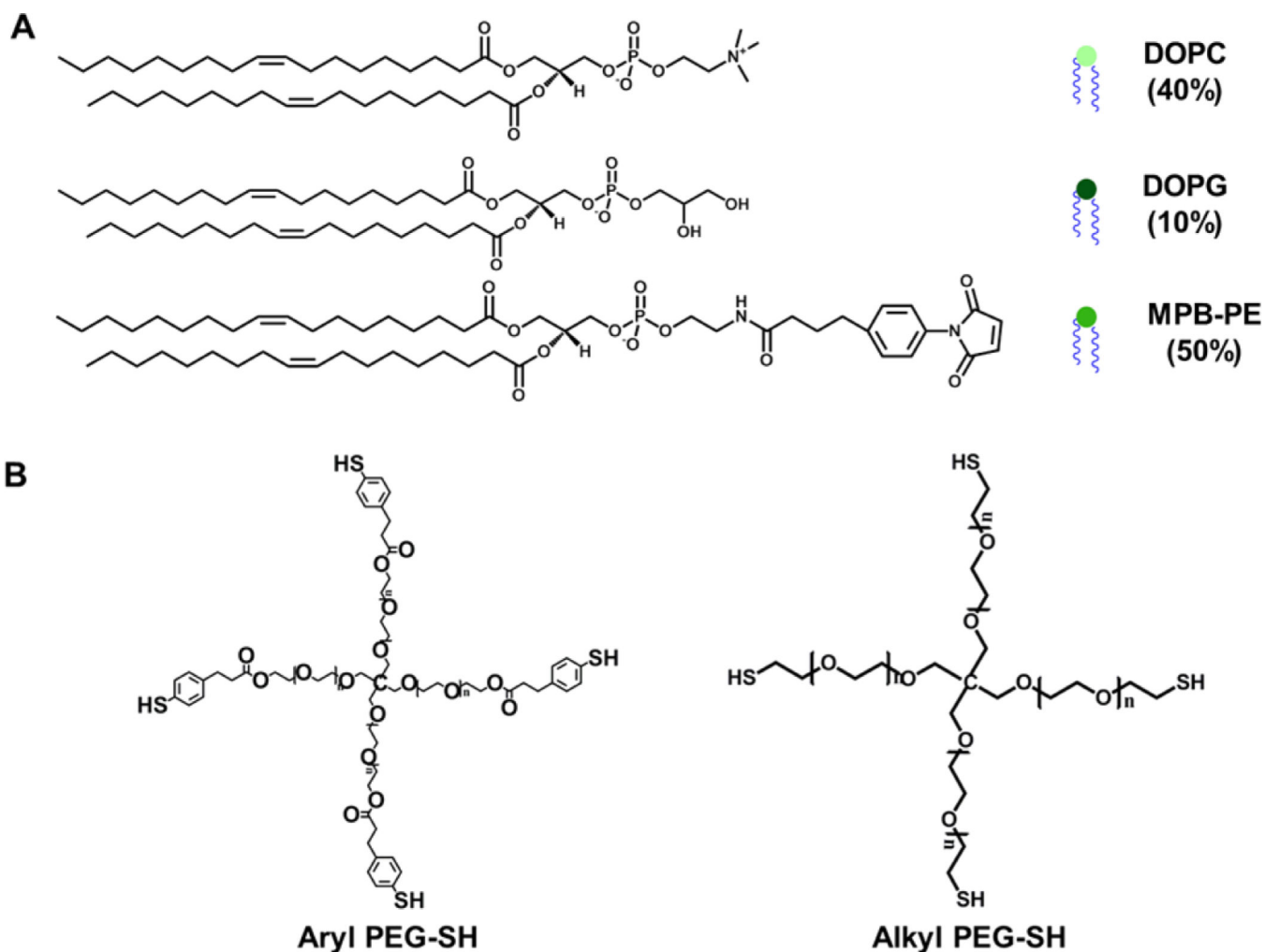
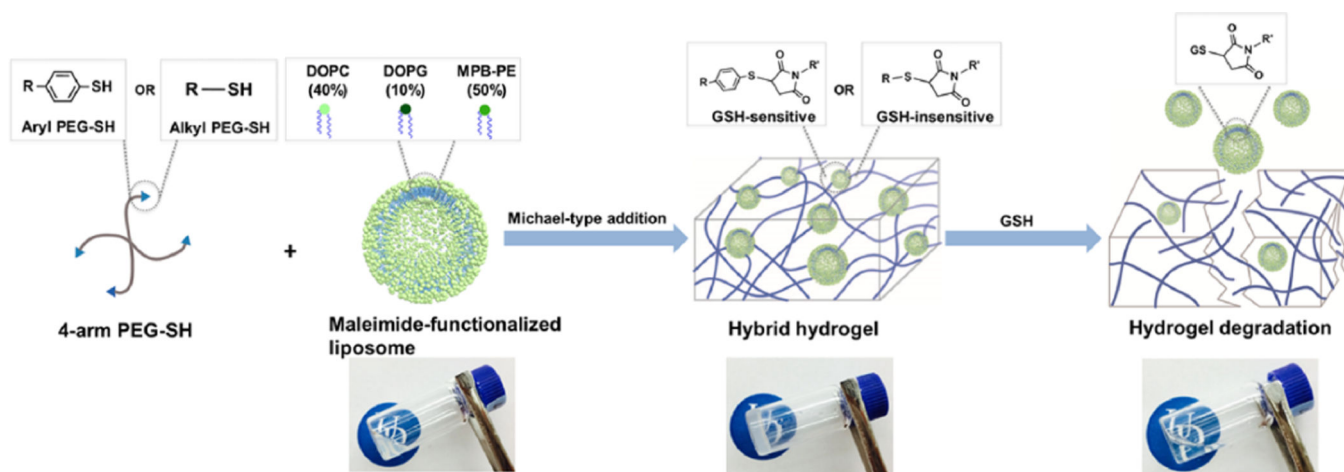


Figure 7.

Release profiles of DOX and cytochrome c from the liposome-cross-linked hydrogels in 10 mM GSH at 37 °C. (A) Co-delivery of DOX and cytochrome c from a single gel. (B) Individual release of DOX and cytochrome c from separate gels (DOX release data replotted from Figure 6). M_t/M_∞ represents the cumulative fractional mass released at time t . Dashed lines indicate the fitted curves of the release profiles. The mean and SD are shown ($n = 3$).



Scheme 1.
 Chemical Structures of the Lipids Used for Liposome Formulation (A) and the PEG-SH Polymers Employed for Hybrid Hydrogel Formation (B)
^aDOPC: 1,2-dioleoyl-*sn*-glycero-3-phosphocholine; DOPG: 1,2-dioleoyl-*sn*-glycero-3-phospho-(1'-*rac*-glycerol); MPB-PE: 1,2-dioleoyl-*sn*-glycero-3-phosphoethanolamine-*N*-[4-(*p*-maleimidophenyl) butyramide].



Scheme 2.
Schematic Representation of the Formation and Degradation of the Liposome Cross-Linked Hybrid Hydrogels

^aThe UD logos are used with permission from the University of Delaware.